



## Degradation of Direct Red 16 using hybrid treatment strategies based on hydrodynamic cavitation, and advanced oxidation processes

Elham Noori<sup>a</sup>, Setareh Eris<sup>a,b</sup>, Fariborz Omid<sup>a</sup>, Sabah Beigrezaee<sup>c</sup>, Anvar Asadi<sup>d,e,\*</sup>

<sup>a</sup>Research Center for Environmental Determinants of Health, School of Public Health, Kermanshah University of Medical Sciences, Kermanshah, Iran, emails: elhamnoori67@gmail.com (E. Noori), omidifariborz@yahoo.com (F. Omid)

<sup>b</sup>Department of Physical Chemistry, Faculty of Chemistry, Bu-Ali Sina University, Hamedan, Iran, email: setare.e123@gmail.com

<sup>c</sup>Students Research Committee, Department of Environmental Health Engineering, Kermanshah University of Medical Sciences, Kermanshah, Iran, email: sbeigrezaee@gmail.com

<sup>d</sup>Environmental Health Research Center, Research Institute for Health Development, Kurdistan University of Medical Sciences, Sanandaj, Iran, email: anvarasadi@muk.ac.ir/anvarasadi@sbcu.ac.ir

<sup>e</sup>Department of Environmental Health Engineering, School of Public Health, Kermanshah University of Medical Sciences, Kermanshah, Iran

Received 9 June 2023; Accepted 12 October 2023

### ABSTRACT

In the present study, the applicability of hydrodynamic cavitation (HC) and its combination with other oxidizing agents including sodium hypochlorite (NaOCl) and UV irradiation for the degradation of Direct Red 16 (DR16) was investigated. The effects of different operating parameters like initial pH (3.0–9.0), different DR16/NaOCl molar ratio (1:20, 1:17, 1:15 and 1:10), initial concentration (20–40 mg/L), and pressure (1.0–5.0 bar) on DR16 degradation were also studied. The combined approaches of HC + UV, NaOCl + UV, HC + NaOCl, and HC + NaOCl + UV were surveyed (under conditions of pH = 6.8, DR16 dosage = 20 ppm, NaOCl/DR16 molar ratio of 20:1, and  $P = 5.0$  bar). The degradation efficiency obtained by the individual processes of HC, UV, and NaOCl were 20%, 17%, and 66%, respectively; while in combined processes of HC + UV, NaOCl + UV, HC + NaOCl, and HC + UV + NaOCl, 42%, 73%, 77% and 88% of DR16 degradation was achieved in tap water, respectively in 30 min of treatment time. Also, for HC + UV + NaOCl process 99% of DR16 degradation was obtained in deionized water. In order to evaluate the kinetics of DR16 degradation, two kinetics models including first order kinetics and fractal like kinetics equations were used. Among the studied kinetics models, fractal like kinetics model showed the best correlation with the experimental data. The obtained data showed that several mechanisms (paths) are involved in DR16 degradation. Based on the obtained results HC + NaOCl + UV can be served as a potential treatment method to degrade dyes and other organic pollutants from aqueous solutions.

**Keywords:** Hydrodynamic cavitation; Direct Red 16; Wastewater; Kinetic; Sodium hypochlorite

### 1. Introduction

Azo dyes are recalcitrant, persistent and non-biodegradable compounds which commonly recognized by the –N = N– band. They are classified as the most widely used

synthetic dyes and toxic pollutants. The carcinogenicity and toxicity of azo dyes make them a serious environmental concern [1]. Direct Red 16 is one the most important azo dyes; it is commonly used for beater dyeing as well as other paper applications. However, highly carcinogenic, mutagenic and strong resistance to biodegradation is reported for

\* Corresponding author.

DR16 [2]. Therefore, it is essential to remove such pollutants from water and other environments with efficient methods [3,4]. Currently, several methods are used for this purpose including adsorption [5], biodegradation [6], flocculation [7], filtration [8], and AOPs [9]. Among the mentioned methods AOPs are more efficient and capable of degrading complex pollutants [10,11]. Some examples of AOP techniques which are used for organic dyes degradation are photo-catalysts, Fenton reagent, photo-Fenton, and cavitation [12,13]. In this regard, cavitation is classified into four types depending on the method of its formation: hydrodynamic, acoustic, optic and particle cavitation. Among these four techniques acoustic (AC) and hydrodynamic cavitation (HC) are known as the most widely used for dyes treatment. However, less energy is consumed when HC is used [14]. HC [15] is a new technology which is used frequently for decomposition of dyes and other complex pollutants. Cavitation reactors operation and design are simple. Moreover, they have capacity for large-scale operations [15]. HC provides various advantages like controllability, low processing time, low energy consumption, and successful targeting. Moreover, this method produces no by-product due to its high oxidative capability [15].

This technology is based on the passing of an aqueous solution through a constriction-diverging device, such as throttling valve, venturi, and orifice plate [16]. During this process, substantial pressure is changed due to the restriction (or modification) of the flow path. If the liquid pressure falls to its vapor pressure (at the operating temperature), cavities are formed and subsequently grown; consequently, the formed cavities are collapsed [13,17]. As a result of the cavities collapse, high localized temperatures of up to 10,000 K and high localized pressures of 101.3 kPa are generated [18]. In such extreme environmental conditions,  $\cdot\text{OH}$  radicals are generated. It is well known that  $\cdot\text{OH}$  radicals have a remarkable ability to oxidize complex pollutants [19]. Furthermore, during the cavities collapse process, the trapped pollutants inside cavities are thermally decomposed/pyrolyzed [20]. However, the use of this process faces an important challenge: the rate of  $\cdot\text{OH}$  radical formation by HC process is low. Several studies reported that HC alone cannot give the required degradation efficiency [21]. Therefore, in many studies, HC is coupled with other techniques such as  $\text{H}_2\text{O}_2$  [22],  $\text{O}_3$  [23], photocatalysts [24], UV irradiation [25], persulfate [26], chlorine compounds [27], activated sodium percarbonate-ozone [28] and etc to provide a hybrid advanced oxidation process in which higher degradation efficiency can be obtained in lesser time. However, a detailed discussion on synergism between HC and different AOPs investigated by Fedorov et al. [29]. There are several papers on the application of HC along with different oxidation processes. In Table 1, we provide a brief literature summary on degradation of containment with HC and combination of HC with other oxidation processes.

As presented in this table and also other studies, many efforts were made to degrade the dyes and other complex components using the combinations of HC and other oxidizing agents. However, to our knowledge, there are no reports on the combination of HC with UV and NaOCl. Therefore, this study aimed at combining the HC and these oxidants to increase the degradation efficiency. For this

purpose, the degradation of DR16 with the use of HC and HC based hybrid advanced oxidation processes such as, HC + UV, HC + NaOCl, and NaOCl + UV, HC + UV + NaOCl processes were studied. As another hybrid approach, the ability of NaOCl + UV in degrading DR16 was investigated. Moreover, the kinetics of the studied processes was investigated by means of first order kinetics and fractal like kinetics models.

## 2. Materials and methods

### 2.1. Materials

DR16 (Table 2) ( $\text{C}_{26}\text{H}_{17}\text{N}_5\text{Na}_2\text{O}_8\text{S}$ ) was obtained from Alvan Co., (Tehran, Iran). Sodium hypochlorite was purchased from Merck (Germany). All chemicals were used without further purification. The pH of the solutions was adjusted by NaOH and HCl (1 M) solutions.

### 2.2. HC reactor setup

The HC reactor setup, used in this study, is schematically represented in Fig. 1. The main parts of the setup are as follows: a holding tank of 20 L volume, reciprocating pump of power rating of 1.1 kW, control valves (V1, V2, and V3), pressure gauges (P1, P2), cavitating device and etc. The venturi geometry (Fig. 1) was selected from the work by Bashir et al. [39]. Therefore, to obtain the best cavitation activity, degradation experiments were performed using a venturi with optimized geometry recommended in their work [39]. There are two pipelines in setup including the main line and bypass line. The cavitating device was accommodated in the main line for generation cavities. The main line pressure and flow were adjusted through control valves in the bypass line. A UV-C lamp (8 W) was applied as the light source. The contaminated water was poured into the feed tank (holding tank) and then it moves into the cavitation region and finally the treated solution returned to the tank again.

### 2.3. Experiment procedures

Degradation of DR16 was carried out using HC at different conditions with a fixed volume of solution (3.0 L) of a known concentration. Tap water was used for preparation of the solutions. For all experiments, the reaction time was set as 5.0, 10, 20, and 30 min and samples were withdrawn at these time intervals for further analysis. The temperature inside the reactor was kept constant at  $30^\circ\text{C} \pm 2^\circ\text{C}$  using a water-cooling jacket.

Hydrodynamic-cavitation-based degradation of DR16 was carried out at different conditions. The effect of initial DR16 concentration on degradation rate was investigated in range of 20–40 mg/L. Furthermore, to investigate the effect of the solution pH, a series of experiments were performed over the pH range of 3.0 to 9.0. Also, four different DR16/NaOCl molar ratios (1:20, 1:17, 1:15 and 1:10) were used to study the effect of NaOCl on DR16 degradation efficiency. The degradation of DR16 was measured by following the decrease in absorbance at 506 nm on a Shimadzu-1800 UV spectrophotometer. All experiments were repeated three times and the average was reported.

Table 1  
Recent applications of HC in combination with other AOPs for degradation of different pollutants

Methodology	Pollutant	Experimental Conditions	Results	References
- HC + (TiO <sub>2</sub> /Er <sup>3+</sup> :YAlO <sub>3</sub> ) + NiFe <sub>2</sub> O <sub>4</sub> -light - HC + TiO <sub>2</sub> + light - HC + NiFe <sub>2</sub> O <sub>4</sub> + light - HC alone	Oxytetracycline	(TiO <sub>2</sub> /Er <sup>3+</sup> :YAlO <sub>3</sub> )/NiFe <sub>2</sub> O <sub>4</sub> = 1 g/L T = 40°C Xenon lamp light source = 300 W Orifice plate = 4 mm	Photocatalyst degradation: (TiO <sub>2</sub> /Er <sup>3+</sup> :YAlO <sub>3</sub> )/NiFe <sub>2</sub> O <sub>4</sub> -light = 84.45% HC + TiO <sub>2</sub> + light = 59.16% HC + NiFe <sub>2</sub> O <sub>4</sub> + light = 52.21% HC alone = 33.99%	[30]
- D-2 - D-3 - D-4	Rhodamine B	Orifice plate = 4 mm Hole diameter = 2 mm T = 40°C	Rhodamine B degradation: D-2 = 46.12%, D-3 = 52.27% D-4 = 31.20%	[31]
Remark: The arrangement of orifice plates and by-pass line is different for D-2, D-3 and D-4				
- HC/K <sub>2</sub> FeO <sub>4</sub> - K <sub>2</sub> FeO <sub>4</sub> -only	Leachate	- Perforated plate = 5 mm Outer diameter = 45 mm Hole diameter = 1.5 mm T = 35°C–38°C - K <sub>2</sub> FeO <sub>4</sub> = 1.5 g/L	COD decrease: - HC/K <sub>2</sub> FeO <sub>4</sub> = 51.69 - K <sub>2</sub> FeO <sub>4</sub> = 40.03%	[32]
- HC - HC + potassium persulfate (KPS) - HC + potassium persulfate + H <sub>2</sub> O <sub>2</sub>	Tartrazine Ponceau 4R Coomassie Brilliant Blue	Thickness of orifice plate = 5 mm Hole diameter = 4 mm T = 30°C ± 2.0°C KPS = 750 mg/L H <sub>2</sub> O <sub>2</sub> = 500 mg/L	Decolorization: Tartrazine: (HC: 16.36%; HC + KPS: 27.30%; HC + KPS + H <sub>2</sub> O <sub>2</sub> : 50.10%) Ponceau 4R: (HC: 14.12%; HC + KPS: 20.68%; HC + KPS + H <sub>2</sub> O <sub>2</sub> : 42.30%) Coomassie Brilliant Blue: (HC: 45.77%; HC + KPS: 68.66%; HC + KPS + H <sub>2</sub> O <sub>2</sub> : 92.27%)	[33]
- Fenton/hydrodynamic cavitation-based packed bed reactor - H <sub>2</sub> O <sub>2</sub> /hydrodynamic cavitation-based packed bed reactor	Methyl Violet 2B	Fenton ratio = 0.6 H <sub>2</sub> O <sub>2</sub> = 265 ppm Diameter of the orifice = 0.2 cm Diameter of the pipe = 10 cm	Methyl Violet 2B degradation: - Fenton/hydrodynamic cavitation-based packed bed reactor 100% - H <sub>2</sub> O <sub>2</sub> /hydrodynamic cavitation-based packed bed reactor 99.6%	[34]
- HC - persulfate - oxalic acid - periodate - HC - oxalic acid (OA) - HC - persulfate (PS) - HC - periodate (PI) - HC alone	Direct Red 89	OA = 100 mg/L PS = 125 mg/L PI = 150 mg/L Diameter of the throat = 0.5 mm Total length = 130 mm T = 25°C–29°C	Direct red 89 removal: - HC - PS - OA - PI = 99.90 ± 0.09% - HC/OA = 78.77 ± 2.36% - HC/PS = 77.13 ± 3.86%, - HC/PI = 95.94 ± 0.96% - HC alone = 56.88 ± 1.7	[35]

Table 1 (Continued)

Table 1

Methodology	Pollutant	Experimental Conditions	Results	References
HC/O <sub>3</sub> /H <sub>2</sub> O <sub>2</sub>	Algae	Cavitation tube, orifice plate distance: 25 cm O <sub>3</sub> value: 3 g/h H <sub>2</sub> O <sub>2</sub> concentration: 2 g/l α-Fe <sub>2</sub> O <sub>3</sub> = 181.82 mg/L	Melosira degradation = 38.16% Oscillatoria degradation = 35.76%	[36]
- HC/persulfate/α-Fe <sub>2</sub> O <sub>3</sub> - HC alone	Sulfadiazine	Na <sub>2</sub> S <sub>2</sub> O <sub>8</sub> = 348.49 mg/L H <sub>2</sub> O <sub>2</sub> = 0.95 ml/L Hole diameter = 2 mm Number of holes = 4	Sulfadiazine degradation - HC/persulfate/α-Fe <sub>2</sub> O <sub>3</sub> = 93.07% - HC alone = 8.26%	[37]
Remark: The aim of the mentioned study was to optimize the design of HC reactor using various orifice plates. However, the best obtained results are re-reported here. - Alone HC - HC + NaOCl	Rhodamine B	Orifice plate: 33 holes of 2 mm diameter NaOCl: 4 mg/L	Degradation: - Alone HC = 8.6% - HC + NaOCl (4 mg/L) = 93.6%	[38]

2.4. Degradation kinetics studies

One of the most important parts of HC processes is kinetics studies. The study of HC kinetics can bring vital information about the mechanism and rate of the process. In order to analyze the kinetics of the DR16 degradation process, none-linear form of two models including first order, and fractal like kinetics models were used [40,41]. The mathematical forms of these models are shown as Eqs. (1), and (2), respectively:

$$C = C_0 \exp(-k_1 t) \tag{1}$$

$$C = C_0 \exp(-k_f t^\alpha) \tag{2}$$

where C and C<sub>0</sub> are the concentration at time 't' and 't = 0', respectively. Also, k<sub>1</sub> and k<sub>f</sub> are the rate coefficient of the first order kinetics and fractal like kinetics models, respectively. Furthermore, α (0 ≤ α ≤ 1) is the fractional time index. This parameter is an indication of the number pathways which are participated in degradation. The further it is from 1, the number of involved paths (in degradation) increases [41].

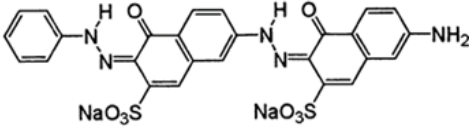
However, the agreement between the experimental data and these kinetics models was evaluated by the correlation coefficients (R<sup>2</sup>). The obtained results from the kinetics model were summarized in Tables 2-4 and S1-S3. The best correlation coefficients were seen for fractal like kinetics model. According to this model, with passing time, different paths appear for DR16 degradation [41]. These paths are including direct degradation of DR16 and radical pathway. It should be mentioned that the obtained correlation coefficients from the first order kinetics model are very lower than that of fractal like kinetics model. Therefore, the fitted parameters of first order kinetics are summarized in supporting information file.

3. Results and discussion

3.1. Effect of initial DR16 concentration

In order to evaluate the effect of initial dye concentration on the degradation rate, experiments were carried out with various initial DR16 concentrations (20-40 mg/L). In all experiments, the operating conditions were pH = 6.8, inlet pressure = 5.0 bar, DR16/NaOCl molar ratio of 1:20. Fig. 2a shows the influence of initial DR16 concentration on degradation efficiency; as can be seen, for all initial concentrations the degradation efficiency was increased as time prolongs. About 88%, 80%, and 75% DR16 degradation was obtained for 20, 30, and 40 ppm of dye concentration, respectively, after 30 min treatment time. Therefore, the degradation efficiency was decreased as the initial dye concentration increased. This can be explained as follow: the experiments of this section were conducted at same operating conditions but different concentrations of DR16. However, the number of generated •OH radicals is only dependent on operating conditions. Therefore, the amount of generated •OH radicals remains constant in all experiments. Hence, by increasing the concentration of DR16, the ratio of •OH radicals to dye molecules was reduced which leads to the decline of degradation efficiency.

Table 2  
DR16 structure and properties

Structure	Properties
	Double azo class, soluble in water for product red, slightly soluble in ethanol peach pink, insoluble in other organic solvents. Molecular weight: 637.55 g/mol

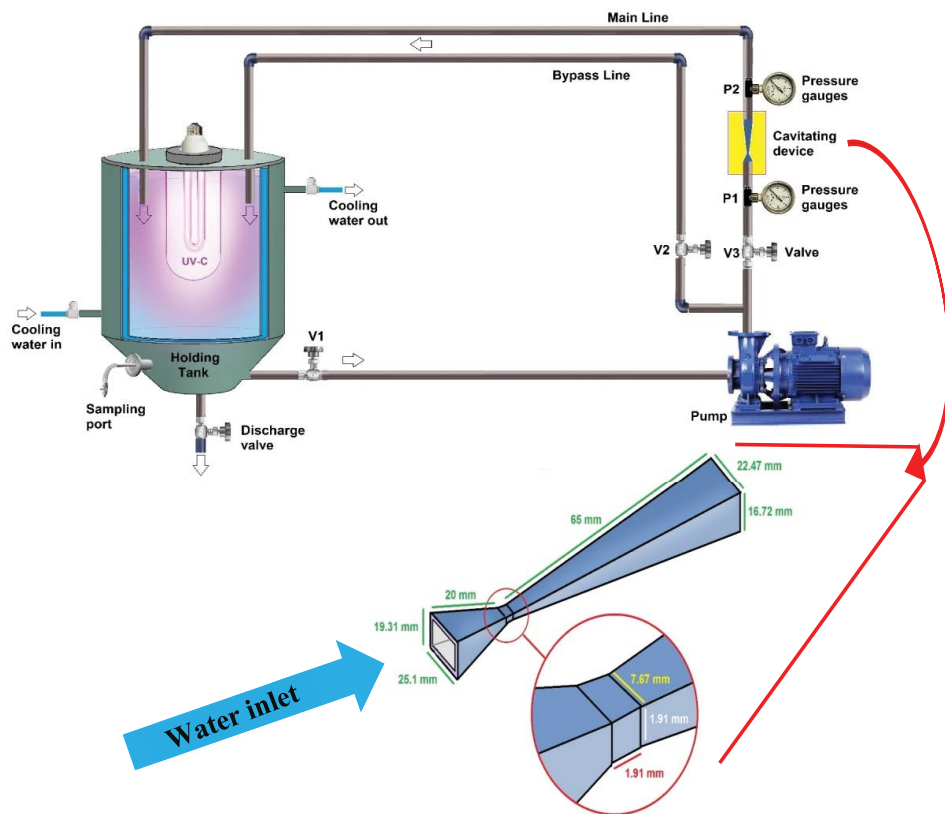


Fig. 1. Schematic view of HC reactor and dimensions of the venturi as the cavitating agent.

Table 3  
Fitted parameters of fractal like kinetics model for degradation of DR16 (with different initial concentrations). Also, the last column shows the degradation efficiency

$C_0$ (mg/L)	$k_f$ (1/min $^\alpha$ )	$\alpha$	$R^2$	Degradation efficiency (%)
20	0.41	0.48	0.9999	88
30	0.39	0.41	0.9996	80
40	0.34	0.39	0.9936	75

For all concentrations, the correlation coefficient of fractal like kinetics model was higher than 0.99 and rate coefficients were 0.39, 0.41, and 0.48, respectively for 40, 30, and 20 ppm. Also, as the initial concentration increased the value of  $\alpha$  decreased. This shows that increasing the

Table 4  
Fitted parameters of fractal like kinetics model for degradation of DR16 at different pH. Also, the last column shows the degradation efficiency

pH	$k_f$ (1/min $^\alpha$ )	$\alpha$	$R^2$	Degradation efficiency
3.8	0.49	0.47	0.9998	92
4.8	0.45	0.48	0.9997	91
5.8	0.44	0.43	0.9991	90
6.8	0.41	0.48	0.9999	88
7.8	0.32	0.52	0.9985	83
8.8	0.28	0.54	0.9924	81

initial concentration of DR16 will increase the number of paths. The fitting parameters for the studied kinetics models are summarized in Table 3. Fig. 2b (symbols) shows

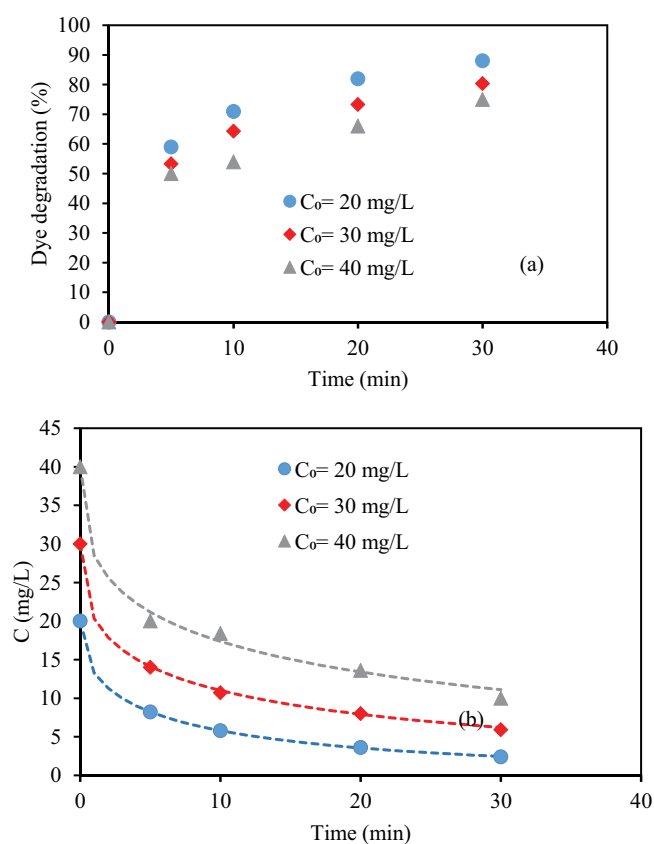


Fig. 2. (a) Effect of initial concentration of DR16 on degradation efficiency. (b) The variation of DR16 concentrations as a function of time at different concentrations the symbols are experimental values and dashed lines are the predicted values by fractal like kinetics model.

the variation of DR16 concentration as function of time. Moreover, the obtained results from the fitting of data using first order kinetics models are shown in Table S1.

### 3.2. Effect of solution pH

One of the most important influencing parameters concerning the feasibility of DR16 degradation is the pH of the solution. The effect of solution pH was studied in the range of 3.8–8.8. The obtained data are shown in Fig. 3a. Moreover, the data were correlated by means of first order kinetics and fractal like kinetics models, and the results are presented in Fig. 3b. Also, the fitting parameters for the studied kinetics models are summarized in Tables 4 and S2. As can be seen from the results, DR16 degradation efficiency and fractal like rate coefficients are decreased with increasing pH. The variation of  $\alpha$  with pH is an indication of different radical species formation at different pH (the existence of different radical will change the number of degradation paths). This observation can be interpreted as follows: in  $\text{pH} < \text{p}K_a$ , dye occurs in neutral form and behaves as a hydrophobic solute [42]. Therefore, at such pH, DR16 has tendency to enter the region of gas–water interface of cavities. Clearly, in this region dye molecules are more readily subjected to radical attacks. On the other hand, in  $\text{pH} > \text{p}K_a$

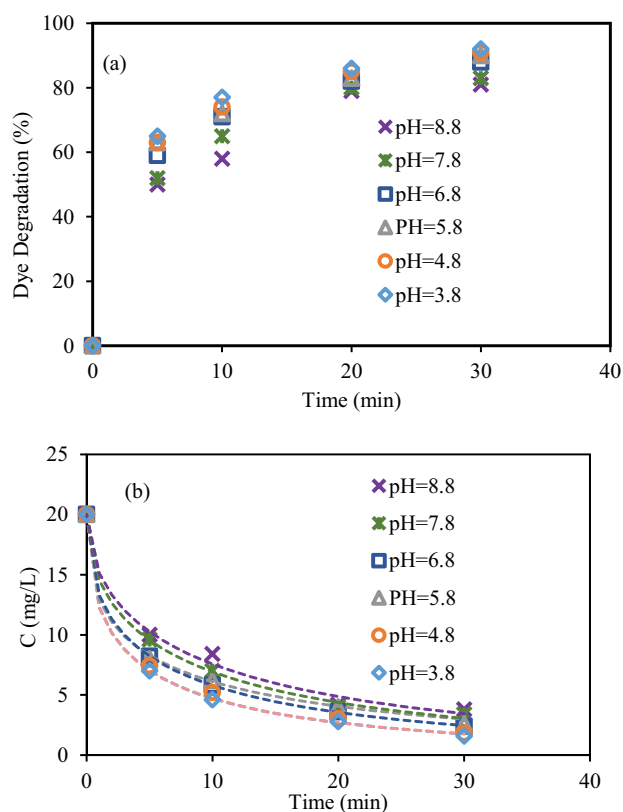


Fig. 3. (a) Effect of the pH on degradation of DR16 at reaction time 30 min, DR16/NaOCl molar ratio of 1:20 and DR16 concentration of 20 ppm under UV irradiation. (b) The variation of DR16 concentrations as a function of time at different pH; the symbols are experimental values and dashed lines are the predicted values by fractal like kinetics model.

dye molecules are in their ionized form and have more affinity to remain in the bulk liquid. It is well known that only about 10% of the hydroxyl radicals (which are generated on the cavity's inner surface) are able to diffuse into the bulk solution [15]. Therefore, lower concentration of hydroxyl radicals leads to lower degradation [15]. Moreover, in aqueous solution,  $\text{OCl}^-$  ion is in equilibrium with hypochlorous acid (HOCl) [38]. However, distribution of species in equilibrium is strongly dependent on solution pH; at the pH range of 2–7 the equilibrium favors hypochlorous acid. The equality exists between HOCl and  $\text{OCl}^-$  at pH of 7.4. The main species is  $\text{Cl}_2$ , when pH is below 2. Therefore, at pH of 3.8, the dominant species is the strongly oxidizing HOCl [38]. According to the literature, un-dissociated HOCl can evaporate into cavitation bubbles where sonolysis of HOCl may occur [43]. Also, more  $\cdot\text{OH}$  radicals are generated in presence of HOCl which results in increase of degradation percentage [44].

Khajeh et al. [42] investigated the degradation of direct red 89 in the pH ranging from 2.2 to 8.2 using HC. They found that under acidic conditions, HC promotes the formation of  $\cdot\text{OH}$  radicals, which have a higher oxidation potential. However, under basic conditions, the presence of hydroxyl ions leads to the recombination of free radicals, resulting in the formation of  $\text{H}_2\text{O}_2$  with lower oxidation capacity.

### 3.3. Effect of NaOCl dosage

Inorganic chlorinated compounds are recognized as one of the strongest oxidative species which are used to degrade organic and other pollutants in water. Sodium hypochlorite can be stored and transported more easily and safely than several other oxidative materials [45]. For example,  $H_2O_2$  as one of the oxidizing agents should be diluted during transport, as a safety measure. While, for oxidation with hydrogen peroxide, high concentrations are required. Moreover, NaOCl is seen to be more economical and applicable ones when compared with other inorganic oxidants [44]. Hence, NaOCl was applied in this study to assess the effect of an oxidant on HC degradation of DR16. For this purpose, different concentrations of DR16/NaOCl molar ratio, ranging from 1:10 to 1:20, were tested. The experiments were performed in conditions of pH 6.8 and DR16 concentration of 20 ppm under UV irradiation. As can be seen in Fig. 4, the degradation efficiency of DR16 was found to increase with increase in concentration of NaOCl. As explained in the previous section, the enhancement of DR16 degradation can be caused by HOCl formation and also by generation of additional  $\cdot OH$  radicals [38]. However, at the minimum DR16/NaOCl molar ratio (1:10), 68% of DR16 degradation was obtained. Also, about 88% DR16 was degraded at the maximum DR16/NaOCl molar ratio (1:20) within 30 min.

### 3.4. Effect of HC inlet pressure

Among the influencing parameters on the hydrodynamic-cavitation-based degradation process, inlet pressure is perhaps the most important one. There is dependence between the inlet fluid pressure and the velocity at the throat; and the cavitating condition in the venture is affected by it [15]. Therefore, to obtain the maximum cavitation effect, optimization of inlet pressure is of paramount importance. In this study, the effect of inlet pressure on the degradation of DR16 was investigated by varying the pressure in the range of 1–5 bars. The experiments were conducted at the same operating condition (DR16 concentration, DR16/NaOCl molar ratio, and the solution pH were 20 mg/L, 1:20, and 6.8, respectively) but different inlet pressure. The results

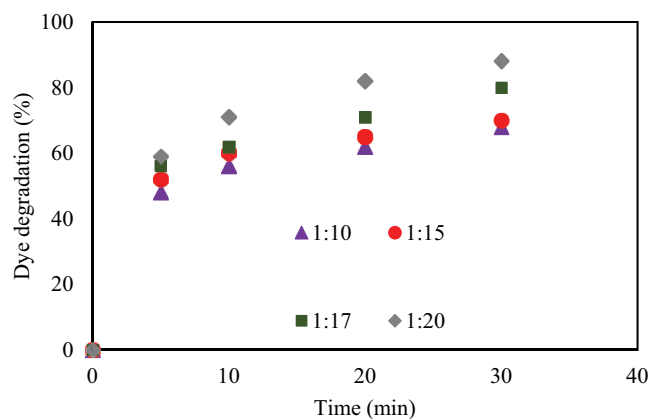


Fig. 4. Effect of the dye/NaOCl molar ratio on the degradation of DR16 (pH = 6.8 and DR16 concentration = 20 ppm under UV irradiation).

(Fig. 5) show that with the increasing pressure to 5 bar, DR16 degradation efficiency was increased. In fact, when the inlet pressure increased, flow rate in the main line (which housed the cavitating device) was increased. As a result, the liquid passes through the venture more times. With increasing the number of passes, the solution will experience the cavitating condition for longer duration [46]. Therefore, cavitation yield and as a result DR16 degradation efficiency was increased. Similar results have been shown in other research. Saharan et al. [15] reported that the degradation of Acid Red 88 increased with an increase in inlet pressure, reaching its maximum at 5 bar inlet pressure, and then decreased.

### 3.5. Synergistic effect study

As reported in many literature [47–50], by combining HC with other oxidants and AOPs, the ability of the process in generating  $\cdot OH$  radicals is enhanced significantly. Here, the effect of HC combined with chemical oxidation processes, including NaOCl and UV irradiation, on DR16 degradation was investigated. However, when HC alone was applied, only 20% of DR16 degradation was obtained. However, to survey the combined effect of HC, NaOCl, and UV on DR16 degradation, a series of experiments were conducted. The kinetics data for the studied methods was correlated by means of first order kinetics and fractal like kinetics equations and the results are listed in Table 5 (for fractal like kinetics model) and Table S3 (for first order kinetics model). The best correlation coefficient was obtained using fractal like kinetics model ( $R^2 > 99\%$ ). In accordance with experimental data, the tendency of fractal like rate coefficient was obtained as follow:  $UV < HC < HC + UV < NaOCl < UV + NaOCl < HC + NaOCl < HC + UV + NaOCl$ . Moreover, the obtained value of  $\alpha$  shows there are several paths for dye degradation. Several kinds of radicals are formed during the processes. Also, the processes themselves can directly degrade DR16. Therefore, it can be said that DR16 degraded in several ways.

#### 3.5.1. HC + NaOCl effect

Sodium hypochlorite is a bleaching agent which commonly employed to treat wastewater. The combined process

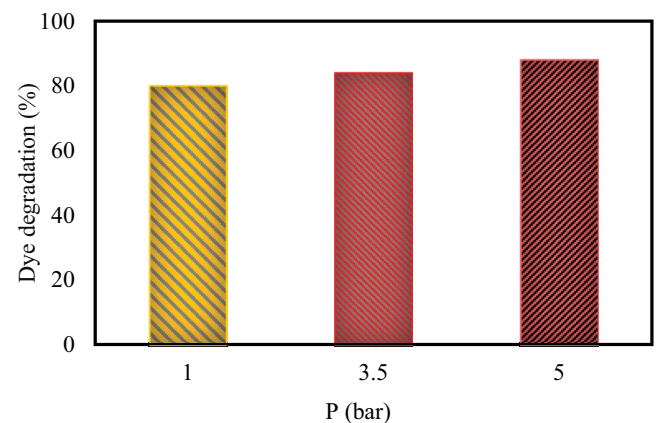


Fig. 5. Effect of pressure on the degradation of DR16 (reaction time of 30 min DR16/NaOCl molar ratio of 1:20, pH = 6.8, and DR16 concentration of 20 ppm under UVC irradiation).

of HC coupled with NaOCl was studied under experimental conditions of pH 6.8, DR16 concentration 20 ppm, NaOCl/DR16 molar ratio of 20:1, and  $P = 5.0$  bars. However, the obtained results are illustrated in Fig. 6a. The results show that the individual use of NaOCl in the degradation of DR16 was resulted in 66% of degradation. However, NaOCl will exhibit more efficiency in DR16 degradation when it is used in combination with HC. Moreover, from the obtained results, it can be concluded that using the hybrid process of HC and NaOCl increases the degradation rate (Fig. 6). The fractal like rate coefficient for individual NaOCl and HC processes were  $0.28 \text{ 1/min}^\alpha$  and  $0.05 \text{ 1/min}^\alpha$ , respectively. However, the rate coefficient was increased to  $0.35 \text{ 1/min}^\alpha$  by the hybrid approach. On the basis of obtained fractal like kinetics rate coefficient, the synergistic index ( $F_{(\text{HC}+\text{NaOCl})}$ ) was calculated by [Eq. (3)]:

$$F_{(\text{HC}+\text{NaOCl})} = \frac{k_{(\text{HC}+\text{NaOCl})}}{k_{\text{HC}} + k_{\text{NaOCl}}} \quad (3)$$

The obtained value was 1.41 which confirmed the synergism between HC and NaOCl. As mentioned before, in the studied pH range the dominant species of  $\text{OCl}^-$  is HOCl. Also, HOCl can promote degradation efficiency through the following ways: sonolysis of undissociated HOCl in cavitation bubble [43] and also producing more  $\cdot\text{OH}$  radicals

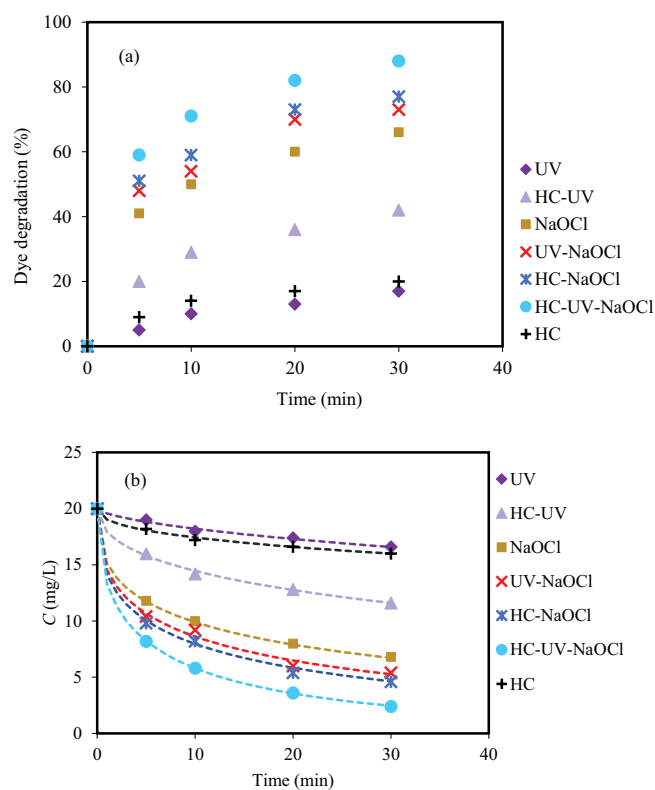


Fig. 6. (a) Comparison of combined treatment of HC, UV and NaOCl in terms of the extent of degradation of DR16 and (b) the variation of DR16 concentrations as a function of time in different processes (pH = 6.8, DR16 dosage = 20 ppm, DR16/NaOCl molar ratio of 1:20,  $P = 5$  bar).

[43,44]. Therefore, it can be said that the synergistic effect between HC and NaOCl for the degradation of DR16 can be mainly attributed to the contribution of additional  $\cdot\text{OH}$  radicals production [38].

Mancuso et al. [38] investigated the synergistic effect between HC and NaOCl in the degradation of RhB. The combined process of HC and NaOCl (at a concentration of  $0.5 \text{ mg/L}$ ) increased the efficiency of RhB degradation by approximately 45%-50% after 260 passes (equivalent to 169 min of operation time) compared to HC alone.

### 3.5.2. UV + NaOCl effect

Photolysis by direct UV irradiation is a promising technology for water disinfection. However, complete degradation of organic pollutants and water treatment cannot be obtained when this method is used alone [44]. As shown in Fig. 6a, when the DR16 solution was treated using UV irradiation and after 30 min only 17% of DR16 was degraded. In fact, DR16 can be photolyzed directly by UV light. Also, UV irradiation leads to the production of dye radicals which are susceptible to further degradation [51]:



However, it is clear that UV radiation alone cannot efficiently be applied to the degradation of DR16. There are several studies which attempted to combine UV irradiation with other technologies to increase degradation efficacy. Here, UV-NaClO photooxidation process was used to study how the hybridization of two oxidation technologies improves the results obtained by individual processes. DR16 degradation efficiencies by different treatment methods (UV, NaOCl, and UV-NaClO) were shown in Fig. 6a. As can be seen, among these three processes the highest degradation efficiency was achieved for UV-NaClO process (about 73% of degradation). This observation might be due to generation of more  $\cdot\text{OH}$  radicals which are produced from  $\text{H}_2\text{O}$  and HOCl photolysis. As mentioned in the previous section,  $\text{OCl}^-$  is presented as HOCl at the pH of this experiment. It is well-known that photolysis of HOCl can generate OH radicals [Eq. (6)]. Furthermore, under UV irradiation,  $\text{H}_2\text{O}$  is oxidized to OH radicals according to Eq. (5) [44,52,53]:



Moreover, the fractal like kinetics rate coefficients were ( $0.32 \text{ 1/min}^\alpha$ ) for UV/NaOCl in UV ( $0.02 \text{ 1/min}^\alpha$ ) for UV, and ( $0.28 \text{ 1/min}^\alpha$ ) for NaOCl.

In order to survey the efficiency of the combined method (UV + NaOCl) the synergistic coefficient ( $F_{(\text{UV}+\text{NaOCl})}$ ) was calculated based on Eq. (7):

$$F_{(\text{UV}+\text{NaOCl})} = \frac{k_{(\text{UV}+\text{NaOCl})}}{k_{\text{UV}} + k_{\text{NaOCl}}} \quad (7)$$

The calculated synergistic coefficient, 1.07, suggests a synergism between UV and NaOCl.



### 3.5.3. HC + UV effect

The combined effect of UV photolysis and HC on DR16 degradation was studied under experimental conditions of pH = 6.8, 20 ppm of DR16, DR16/NaOCl molar ratio of 1:20, and  $P = 5.0$  bars. The obtained results were shown in Fig. 6a. According to the results, 42% of DR16 degradation was achieved by using the combined treatment of UV + HC; whereas the degradation efficiencies obtained by the individual processes of UV and HC were 17% and 20%, respectively. However, the observed enhancement in DR16 degradation (in the case of UV + HC) can be interpreted:

$H_2O_2$ , which is formed during the cavitation process [Eqs. (8) and (9)], can be cleaved to  $\cdot OH$  radicals from the individual processes of HC and UV are contributed in radicals under UV radiation [Eq. (11)] [54]:



Moreover, the generated  $H_2O_2$  can (oxidize) degrade DR16. Therefore, more number of hydroxyl radicals is available in combined treatment process.

The kinetics data were correlated to the studied kinetics models. However, the obtained fractal like rate coefficients were 0.02 1/min $^{\alpha}$ , 0.05 1/min $^{\alpha}$ , and 0.11 1/min $^{\alpha}$  for UV, HC, and combined HC + UV, respectively. The fractal like rate coefficients were used to calculate the synergistic index according to Eq. (11):

$$F_{(HC+UV)} = \frac{k_{(HC+UV)}}{k_{HC} + k_{UV}} \quad (11)$$

The obtained value for synergistic index was 1.57 which confirmed the synergism of HC with UV.

Cako et al. [55] investigated the effect of the hybridization treatment approach of HC/UV on Brilliant Cresyl Blue degradation. They achieved a degradation extent of 34% using the combination of HC with UV irradiation, whereas only 10% and 22% degradation were obtained with the individual process of HC and UV, respectively.

Table 5

Fitted parameters of fractal like kinetics model for degradation of DR16 with different processes of HC, UV, NaOCl, HC + UV, HC + NaOCl, UV + NaOCl and HC + UV + NaOCl

Method	$k_f$ (1/min $^{\alpha}$ )	$\alpha$	$R^2$
HC	0.05	0.44	0.993
UV	0.02	0.63	0.988
NaOCl	0.28	0.40	0.999
HC + UV	0.11	0.47	0.997
HC + NaOCl	0.35	0.42	0.998
UV + NaOCl	0.32	0.42	0.995
HC + UV + NaOCl	0.41	0.48	0.999

### 3.5.4. HC + UV + NaOCl effect

The performance of the combination approach of HC, UV, and NaOCl was also surveyed for the degradation of DR16. The obtained results for the degradation of DR16 over the treatment time are shown in Fig. 6a. As can be seen in this figure the combination of UV, HC, and NaOCl (DR16/NaOCl molar ratio of 1:20) resulted in 88% of DR16 degradation which is the highest degradation efficiency amount among the tested processes. Moreover, fractal like rate coefficient for this process was found to be 0.41 1/min $^{\alpha}$ . The synergetic effect of this process was calculated on the ground of Eq. (12):

$$F_{(HC+UV+NaOCl)} = \frac{k_{(HC+UV+NaOCl)}}{k_{HC} + k_{UV} + k_{NaOCl}} \quad (12)$$

The obtained value of  $F_{(UV+HC+NaOCl)}$  1.17, shows that there is a synergism between UV, HC, and NaOCl. The observed synergism can be explained as follow: as mentioned above, each of UV, HC, and NaOCl was found to affect the degradation process individually. Also, NaOCl can be dissociated under UV irradiation. Moreover, cavitation effects assist in intensifying the dissociation of NaOCl. Therefore, higher degradation was observed in the hybrid process of UV + HC + NaOCl.

As mentioned before, tap water is used in all experiments. However, to investigate the effect of anions and water matrix, an experiment was performed with deionized water and the obtained results are present in Fig. S1. As can be seen in this figure when deionized water is used, the degradation efficiency increased. This observation shows that the presence of ions in tap water can decrease the oxidant and subsequently the degradation efficiency.

Askarniya et al. [33] investigated decolorization of tartrazine, ponceau 4R, and coomassie, brilliant blue using hybrid process of HC-KPS- $H_2O_2$ . A synergetic coefficient of 2.51 was achieved by HC-KPS- $H_2O_2$  which proved the effectiveness of the process.

Çalışkan et al. [56] studied the degradation of high concentrated azo dye solutions using an innovative hybrid process of HC and photocatalysis in a pilot reactor. They investigated HC, HC + photocatalyst, HC + UV processes for RR180 decolorization. They found that HC + photocatalyst exhibited better mineralization at an inlet pressure of 5 bar compared to individual processes of HC. The synergetic coefficients for TOC and COD removal were found to be 1.17 and 1.48, respectively.

### 3.5.5. Comparison with other treatment of DR16

There are other processes which are used to degrade DR16. In this section, a comparison was provided between HC + NaOCl + UV process and some of other reported processes. The results are summarized in Table 6. In all of these studies deionized water was used as solvent. In comparison with other methods, HC + NaOCl + UV process has several advantages:

- The degradation time in HC + NaOCl + UV process is much smaller than that of other reported processes.

Table 6  
Comparison of HC + NaOCl + UV process efficiency with other DR16 process type

Process type	Reaction conditions	Removal	References
Photocatalyst (Ag-TiO <sub>2</sub> /PW/surfactant)	Time = 2 h, DR16 concentration 25 ppm, pH = 5 and catalyst loading 1 g/L, visible light (18 W fluorescent lamp)	94%	[2]
Photocatalyst (11-KPW/TiO <sub>2</sub> )	Time = 4 h, DR16 concentration = 20 ppm, pH = 3 and catalyst loading 1.25 g/L, visible light (LED lamp)	98%	[57]
Photocatalyst (p-CuFeO <sub>2</sub> /n-ZnO)	Time = 210 min, visible light, DR16 concentration = 50 ppm, visible light (tungsten-halogen lamp (200 W, Phillips)	84% (mineralization)	[58]
Photocatalyst (PMoWSn/TiO <sub>2</sub> )	Time = 210 min, DR16 concentration 20 ppm, pH = 3, catalyst loading = 1 g/L, visible light (LED lamp)	94%	[59]
(HC-UV-NaOCl)	Initial concentration = 20 ppm, temperature = 30°C, contact time = 30 min, P = 5 bar	99%	Present work

- More degradation efficiency was obtained using HC + NaOCl + UV process
- The degradation was carried out in semi-industrial scale
- The HC + NaOCl + UV process has economical advantage.

#### 4. Conclusion

This work aimed at DR16 degradation based on the HC treatment process in combination with NaOCl and UV irradiation as a three simple, green and effective treatment methods. Compared to other treatment methods, they are favored due to their economic aspects, ease of use, scalability, and promising results. It is found that combining HC with various AOPs is more effective than using each technique alone since the combination produces more OH<sup>-</sup> radicals, which intensifies the degradation and mineralization. The HC + UV + NaOCl approach was found to be the most effective combination, and DR16 degradation of 88% was obtained by applying this method. At the same experimental conditions, HC, UV, NaOCl, HC + NaOCl, HC + UV, and NaOCl + UV were resulted in 20%, 17%, 66%, 77%, and 42% and of DR16 degradation, respectively. The degradation of the DR16 through HC process was increased with an increase in inlet pressure till 5.0 bar.

For DR16 degradation, fractal like rate coefficient of 0.02 1/min<sup>α</sup>, 0.05 1/min<sup>α</sup>, 0.11 1/min<sup>α</sup>, 0.28 1/min<sup>α</sup>, 0.32 1/min<sup>α</sup>, 0.35 1/min<sup>α</sup>, and 0.41 1/min<sup>α</sup> was obtained using UV, HC, HC + UV, NaOCl, UV + NaOCl, HC + NaOCl and HC + UV + NaOCl, respectively. Furthermore, based on the obtained values for α, it can be said that different pathways are involved in DR16 degradation. Moreover, a synergetic coefficient of 1.17, 1.57, 1.41, and 1.07 was achieved by the hybrid processes of HC + NaOCl + UV, HC + UV, HC + NaOCl, and NaOCl + UV, respectively. It is demonstrated that HC-UV-NaOCl is an environmental-friendly, simple to operate, and efficient method to degrade DR16 contaminated wastewater.

#### Funding

The authors gratefully acknowledge the Research Council of Kermanshah University of Medical Sciences (Grant Number: 990814) for the financial assistance.

#### Author contributions

Elham Noori: Data curation, Formal analysis, Methodology, Software, Writing-original draft. Setareh Eris: Formal analysis, Methodology, Visualization, Writing - original draft. Fariborz Omidi: Writing - review & editing. Sabah Beigrezaee: Data curation, Formal analysis, Methodology Anvar Asadi: Project administration, Supervision, Resources, Data curation, Formal analysis, Methodology, Software, Writing - original draft.

#### Declaration of competing interest

The authors declare that they have no known competing financial interests or personal relationships that could have appeared to influence the work reported in this paper.

#### Data availability

The authors confirm that the data supporting the findings of this study are available within the article.

#### Ethics approval

This work was approved under ethical code # IR.KUMS.REC.1399.848.

#### Consent to participate

Not applicable.

#### Consent for publication

Not applicable.

#### Conflict of interests

The authors declare that they have no conflict of interest.

#### References

- [1] Y. Anjaneyulu, N. Sreedhara Chary, D. Samuel Suman Raj, Decolourization of industrial effluents—available methods

- and emerging technologies—a review, *Rev. Environ. Sci. Bio/Technol.*, 4 (2005) 245–273.
- [2] E. Rafiee, E. Noori, A.A. Zinatizadeh, H. Zangeneh, Surfactant effect on photocatalytic activity of Ag-TiO<sub>2</sub>/PW nanocomposite in DR16 degradation: characterization of nanocomposite and RSM process optimization, *Mater. Sci. Semicond. Process.*, 83 (2018) 115–124.
  - [3] R. Al-Tohamy, S.S. Ali, F. Li, K.M. Okasha, Y.A.-G. Mahmoud, T. Elsamahy, H. Jiao, Y. Fu, J. Sun, A critical review on the treatment of dye-containing wastewater: ecotoxicological and health concerns of textile dyes and possible remediation approaches for environmental safety, *Ecotoxicol. Environ. Saf.*, 231 (2022) 113160, doi: 10.1016/j.ecoenv.2021.113160.
  - [4] S. Velusamy, A. Roy, S. Sundaram, T. Kumar Mallick, A review on heavy metal ions and containing dyes removal through graphene oxide-based adsorption strategies for textile wastewater treatment, *Chem. Rec.*, 21 (2021) 1570–1610.
  - [5] L.A. Kafshgari, M. Ghorbani, A. Azizi, S. Agarwal, V.K. Gupta, Modeling and optimization of Direct Red 16 adsorption from aqueous solutions using nanocomposite of MnFe<sub>2</sub>O<sub>4</sub>/MWCNTs: RSM-CCRD model, *J. Mol. Liq.*, 233 (2017) 370–377.
  - [6] Y. Shi, Z. Yang, L. Xing, X. Zhang, X. Li, D. Zhang, Recent advances in the biodegradation of azo dyes, *World J. Microbiol. Biotechnol.*, 37 (2021) 1–18.
  - [7] P.J. Quinlan, A. Tanvir, K.C. Tam, Application of the central composite design to study the flocculation of an anionic azo dye using quaternized cellulose nanofibrils, *Carbohydr. Polym.*, 133 (2015) 80–89.
  - [8] K. Jankowska, Z. Su, J. Zdarta, T. Jesionowski, M. Pinelo, Synergistic action of laccase treatment and membrane filtration during removal of azo dyes in an enzymatic membrane reactor upgraded with electrospun fibers, *J. Hazard. Mater.*, 435 (2022) 129071, doi: 10.1016/j.jhazmat.2022.129071.
  - [9] B. Bhanvase, T. Shende, S. Sonawane, A review on graphene-TiO<sub>2</sub> and doped graphene-TiO<sub>2</sub> nanocomposite photocatalyst for water and wastewater treatment, *Environ. Technol. Rev.*, 6 (2017) 1–14.
  - [10] M. Cheng, G. Zeng, D. Huang, C. Lai, P. Xu, C. Zhang, Y. Liu, Hydroxyl radicals based advanced oxidation processes (AOPs) for remediation of soils contaminated with organic compounds: a review, *Chem. Eng. J.*, 284 (2016) 582–598.
  - [11] M.P. Rayaroth, G. Boczkaj, O. Aubry, U.K. Aravind, C.T. Aravindakumar, Advanced oxidation processes for degradation of water pollutants—ambivalent impact of carbonate species: a review, *Water*, 15 (2023) 1615, doi: 10.3390/w15081615.
  - [12] A.V. Mohod, M. Momotko, N.S. Shah, M. Marchel, M. Imran, L. Kong, G. Boczkaj, Degradation of rhodamine dyes by advanced oxidation processes (AOPs)—focus on cavitation and photocatalysis—a critical review, *Water Resour. Ind.*, 30 (2023) 100220, doi: 10.1016/j.wri.2023.100220.
  - [13] P. Braeutigam, M. Franke, R.J. Schneider, A. Lehmann, A. Stolle, B. Ondruschka, Degradation of carbamazepine in environmentally relevant concentrations in water by hydrodynamic-acoustic-cavitation (HAC), *Water Res.*, 46 (2012) 2469–2477.
  - [14] L. Wang, D. Luo, O. Hamdaoui, Y. Vasseghian, M. Momotko, G. Boczkaj, G.Z. Kyzas, C. Wang, Bibliometric analysis and literature review of ultrasound-assisted degradation of organic pollutants, *Sci. Total Environ.*, 876 (2023) 162551, doi: 10.1016/j.scitotenv.2023.162551.
  - [15] V.K. Saharan, A.B. Pandit, P.S. Satish Kumar, S. Anandan, Hydrodynamic cavitation as an advanced oxidation technique for the degradation of Acid Red 88 dye, *Ind. Eng. Chem. Res.*, 51 (2012) 1981–1989.
  - [16] P.R. Gogate, A.B. Pandit, A review and assessment of hydrodynamic cavitation as a technology for the future, *Ultrason. Sonochem.*, 12 (2005) 21–27.
  - [17] L.P. Amin, P.R. Gogate, A.E. Burgess, D.H. Bremner, Optimization of a hydrodynamic cavitation reactor using salicylic acid dosimetry, *Chem. Eng. J.*, 156 (2010) 165–169.
  - [18] P.B. Patil, A.D. Goswami, N.L. Jadhav, A.J. Sayyed, C.R. Holkar, D.V. Pinjari, Pilot Scale Advance Oxidation Process for Industrial Effluent Treatment, in: *Novel Approaches Towards Wastewater Treatment and Resource Recovery Technologies*, Elsevier, 2022, pp. 471–496.
  - [19] L.V. Malade, U.B. Deshannavar, Decolorisation of Reactive Red 120 by hydrodynamic cavitation, *Mater. Today Proc.*, 5 (2018) 18400–18409.
  - [20] V.K. Saharan, M.P. Badve, A.B. Pandit, Degradation of Reactive Red 120 dye using hydrodynamic cavitation, *Chem. Eng. J.*, 178 (2011) 100–107.
  - [21] M.S. Kumar, S. Sonawane, B. Bhanvase, B. Bethi, Treatment of ternary dye wastewater by hydrodynamic cavitation combined with other advanced oxidation processes (AOP's), *J. Water Process Eng.*, 23 (2018) 250–256.
  - [22] J.P.M. Andia, A.E.T. Cayte, J.M.I. Rodriguez, L.L. Belón, M.A.C. Málaga, L.A.C. Teixeira, Combined treatment based on synergism between hydrodynamic cavitation and H<sub>2</sub>O<sub>2</sub> for degradation of cyanide in effluents, *Miner. Eng.*, 171 (2021) 107119, doi: 10.1016/j.mineng.2021.107119.
  - [23] J. Wang, H. Chen, R. Yuan, F. Wang, F. Ma, B. Zhou, Intensified degradation of textile wastewater using a novel treatment of hydrodynamic cavitation with the combination of ozone, *J. Environ. Chem. Eng.*, 8 (2020) 103959, doi: 10.1016/j.jece.2020.103959.
  - [24] X. Wang, J. Jia, Y. Wang, Combination of photocatalysis with hydrodynamic cavitation for degradation of tetracycline, *Chem. Eng. J.*, 315 (2017) 274–282.
  - [25] P. Thanekar, M. Panda, P.R. Gogate, Degradation of carbamazepine using hydrodynamic cavitation combined with advanced oxidation processes, *Ultrason. Sonochem.*, 40 (2018) 567–576.
  - [26] C.-M. Hung, C.-P. Huang, C.-W. Chen, C.-D. Dong, Hydrodynamic cavitation activation of persulfate for the degradation of polycyclic aromatic hydrocarbons in marine sediments, *Environ. Pollut.*, 286 (2021) 117245, doi: 10.1016/j.envpol.2021.117245.
  - [27] M.P. Badve, M.N. Bhagat, A.B. Pandit, Microbial disinfection of seawater using hydrodynamic cavitation, *Sep. Purif. Technol.*, 151 (2015) 31–38.
  - [28] K. Fedorov, M.P. Rayaroth, N.S. Shah, G. Boczkaj, Activated sodium percarbonate-ozone (SPC/O<sub>3</sub>) hybrid hydrodynamic cavitation system for advanced oxidation processes (AOPs) of 1,4-dioxane in water, *Chem. Eng. J.*, 456 (2023) 141027, doi: 10.1016/j.cej.2022.141027.
  - [29] K. Fedorov, K. Dinesh, X. Sun, R.D.C. Soltani, Z. Wang, S. Sonawane, G. Boczkaj, Synergistic effects of hybrid advanced oxidation processes (AOPs) based on hydrodynamic cavitation phenomenon—a review, *Chem. Eng. J.*, 432 (2022) 134191, doi: 10.1016/j.cej.2021.134191.
  - [30] L. Yi, J. Qin, H. Sun, Y. Ruan, D. Fang, J. Wang, Construction of Z-scheme (TiO<sub>2</sub>/Er<sup>3+</sup>:YAlO<sub>3</sub>)/NiFe<sub>2</sub>O<sub>4</sub> photocatalyst composite for intensifying hydrodynamic cavitation degradation of oxytetracycline in aqueous solution, *Sep. Purif. Technol.*, 293 (2022) 121138, doi: 10.1016/j.seppur.2022.121138.
  - [31] S. Wang, L. Zhao, Y. Ruan, J. Qin, L. Yi, Z. Zhang, J. Wang, D. Fang, Investigation on series-wound orifice plate hydrodynamic cavitation (HC) degradation of Rhodamine B (RhB) assisted by several by-pass line orifice plates, *J. Water Process Eng.*, 51 (2023) 103404, doi: 10.1016/j.jwpe.2022.103404.
  - [32] X. Feng, R. Jin, Y. Qiao, Z. He, J. Liu, Z. Sun, Y. Zhang, M. Jia, J. Gao, A. Wang, A novel process for landfill leachate pretreatment using hydrodynamic cavitation combined with potassium ferrate oxidation, *J. Chem. Technol. Biotechnol.*, 97 (2022) 2537–2546.
  - [33] Z. Askarniya, S. Baradaran, S.H. Sonawane, G. Boczkaj, A comparative study on the decolorization of Tartrazine, Ponceau 4R, and Coomassie Brilliant Blue using persulfate and hydrogen peroxide based advanced oxidation processes combined with hydrodynamic cavitation, *Chem. Eng. Process. Process Intensif.*, 181 (2022) 109160, doi: 10.1016/j.cep.2022.109160.
  - [34] M. Bagal, B. Ramos, S. Mahajan, A. Sonawane, P.H. Palharim, A. Mohod, Parametric optimization of a hybrid cavitation-based Fenton process for the degradation of methyl violet 2B in a packed bed reactor, *Chem. Eng. Res. Des.*, 189 (2023) 440–451.

- [35] M. Khajeh, E. Taheri, M.M. Amin, A. Fatehizadeh, J. Bedia, Combination of hydrodynamic cavitation with oxidants for efficient treatment of synthetic and real textile wastewater, *J. Water Process Eng.*, 49 (2022) 103143, doi: 10.1016/j.jwpe.2022.103143.
- [36] R. Shokooji, A. Rahmani, G. Asgari, M. Ashrafi, E. Ghahramani, Removal of algae using hydrodynamic cavitation, ozonation and oxygen peroxide: Taguchi optimization (case study: raw water of Sanandaj Water Treatment Plant), *Process Saf. Environ. Prot.*, 169 (2023) 896–908.
- [37] K. Roy, V.S. Moholkar, Sulfadiazine degradation by combination of hydrodynamic cavitation and Fenton–persulfate: parametric optimization and deduction of chemical mechanism, *Environ. Sci. Pollut. Res.*, 30 (2022) 25569–25581.
- [38] G. Mancuso, M. Langone, M. Laezza, G. Andreottola, Decolourization of Rhodamine B: a swirling jet-induced cavitation combined with NaOCl, *Ultrason. Sonochem.*, 32 (2016) 18–30.
- [39] T.A. Bashir, A.G. Soni, A.V. Mahulkar, A.B. Pandit, The CFD driven optimisation of a modified venturi for cavitation activity, *Can. J. Chem. Eng.*, 89 (2011) 1366–1375.
- [40] J. Huang, X. Li, M. Ma, D. Li, Removal of di-(2-ethylhexyl) phthalate from aqueous solution by UV/peroxymonosulfate: influencing factors and reaction pathways, *Chem. Eng. J.*, 314 (2017) 182–191.
- [41] E. Noori, S. Eris, F. Omid, A. Asadi, Hybrid approaches based on hydrodynamic cavitation, peroxymonosulfate and UVC irradiation for treatment of organic pollutants: fractal like kinetics, modeling and process optimization, *Environ. Sci. Pollut. Res.*, 30 (2023) 85835–85849.
- [42] M. Khajeh, M.M. Amin, E. Taheri, A. Fatehizadeh, G. McKay, Influence of co-existing cations and anions on removal of Direct Red 89 dye from synthetic wastewater by hydrodynamic cavitation process: an empirical modeling, *Ultrason. Sonochem.*, 67 (2020) 105133, doi: 10.1016/j.ultsonch.2020.105133.
- [43] T.J. Tiong, G.J. Price, Ultrasound promoted reaction of Rhodamine B with sodium hypochlorite using sonochemical and dental ultrasonic instruments, *Ultrason. Sonochem.*, 19 (2012) 358–364.
- [44] Q.-F. Zeng, J. Fu, Y.-T. Shi, H.-L. Zhu, Degradation of CI Disperse Blue 56 by ultraviolet radiation/sodium hypochlorite, *Ozone: Sci. Eng.*, 31 (2009) 37–44.
- [45] A. Siregar, M. Kleber, R. Mikutta, R. Jahn, Sodium hypochlorite oxidation reduces soil organic matter concentrations without affecting inorganic soil constituents, *Eur. J. Soil Sci.*, 56 (2005) 481–490.
- [46] N.P. Vichare, P.R. Gogate, A.B. Pandit, Optimization of hydrodynamic cavitation using a model reaction, *Chem. Eng. Technol.*, 23 (2000) 683–690.
- [47] B. Wang, T. Wang, H. Su, A dye-methylene blue (MB)-degraded by hydrodynamic cavitation (HC) and combined with other oxidants, *J. Environ. Chem. Eng.*, 10 (2022) 107877, doi: 10.1016/j.jece.2022.107877.
- [48] N. Lakshmi, C. Agarkoti, P.R. Gogate, A.B. Pandit, Acoustic and hydrodynamic cavitation-based combined treatment techniques for the treatment of industrial real effluent containing mainly pharmaceutical compounds, *J. Environ. Chem. Eng.*, 10 (2022) 108349, doi: 10.1016/j.jece.2022.108349.
- [49] B. Wang, H. Jiao, H. Su, T. Wang, Degradation of pefloxacin by hybrid hydrodynamic cavitation with H<sub>2</sub>O<sub>2</sub> and O<sub>3</sub>, *Chemosphere*, 303 (2022) 135299, doi: 10.1016/j.chemosphere.2022.135299.
- [50] J. Wang, J. Wang, R. Yuan, J. Liu, Z. Yin, T. He, M. Wang, F. Ma, B. Zhou, H. Chen, Degradation of Acid Red 73 wastewater by hydrodynamic cavitation combined with ozone and its mechanism, *Environ. Res.*, 210 (2022) 112954, doi: 10.1016/j.envres.2022.112954.
- [51] M.A. Tariq, M. Faisal, M. Saquib, M. Muneer, Heterogeneous photocatalytic degradation of an anthraquinone and a triphenylmethane dye derivative in aqueous suspensions of semiconductor, *Dyes Pigm.*, 76 (2008) 358–365.
- [52] S. Li, X. Ao, C. Li, Z. Lu, W. Cao, F. Wu, S. Liu, W. Sun, Insight into PPCP degradation by UV/NH<sub>2</sub>Cl and comparison with UV/NaClO: kinetics, reaction mechanism, and DBP formation, *Water Res.*, 182 (2020) 115967, doi: 10.1016/j.watres.2020.115967.
- [53] N. Rastkari, A. Eslami, S. Nasser, E. Piroti, A. Asadi, Optimizing parameters on nanophotocatalytic degradation of ibuprofen using UVC/ZnO processes by response surface methodology, *Pol. J. Environ. Stud.*, 26 (2017) 785–794.
- [54] X. Wang, J. Wang, P. Guo, W. Guo, C. Wang, Degradation of Rhodamine B in aqueous solution by using swirling jet-induced cavitation combined with H<sub>2</sub>O<sub>2</sub>, *J. Hazard. Mater.*, 169 (2009) 486–491.
- [55] E. Cako, K.D. Gunasekaran, R.D.C. Soltani, G. Boczkaj, Ultrafast degradation of brilliant cresyl blue under hydrodynamic cavitation based advanced oxidation processes (AOPs), *Water Resour. Ind.*, 24 (2020) 100134, doi: 10.1016/j.wri.2020.100134.
- [56] Y. Çalışkan, H.C. Yatmaz, N. Bektaş, Photocatalytic oxidation of high concentrated dye solutions enhanced by hydrodynamic cavitation in a pilot reactor, *Process Saf. Environ. Prot.*, 111 (2017) 428–438.
- [57] E. Rafiee, E. Noori, A.A. Zinatizadeh, H. Zanganeh, A new visible driven nanocomposite including Ti-substituted polyoxometalate/TiO<sub>2</sub>: synthesis, characterization, photo-degradation of azo dye process optimization by RSM and specific removal rate calculations, *J. Mater. Sci.: Mater. Electron.*, 29 (2018) 20668–20679.
- [58] S. Boumazza, F. Kaouah, D. Hamane, M. Trari, S. Omeiri, Z. Bendjama, Visible light assisted decolorization of azo dyes: Direct Red 16 and Direct Blue 71 in aqueous solution on the p-CuFeO<sub>2</sub>/n-ZnO system, *J. Mol. Catal. A: Chem.*, 393 (2014) 156–165.
- [59] E. Rafiee, E. Noori, A. Zinatizadeh, H. Zanganeh, ([n-C<sub>4</sub>H<sub>9</sub>)<sub>3</sub>N]<sub>3</sub>PMo<sub>2</sub>W<sub>9</sub>(Sn<sup>4+</sup>·xH<sub>2</sub>O)<sub>30</sub>/TiO<sub>2</sub>): a new visible photocatalyst for photodegradation of DR16 characterization and optimization process by RSM, *J. Iran. Chem. Soc.*, 18 (2021) 1761–1772.

## Supporting information

Table S1

Fitted parameters of first order kinetics model for degradation of DR16 (at different initial concentration of DR16)

C <sub>0</sub> (mg/L)	k <sub>1</sub> (1/min)	R <sup>2</sup>
20	0.0805	0.8020
30	0.0680	0.7298
40	0.0603	0.7418

Table S2

Fitted parameters of first order kinetics model for degradation of DR16 at different pH

pH	k <sub>1</sub> (1/min)	R <sup>2</sup>
3.8	0.0948	0.8068
4.8	0.0858	0.8109
5.8	0.0903	0.9516
6.8	0.0805	0.8020
7.8	0.0698	0.7930
8.8	0.0645	0.8196

Table S3

Fitted parameters of first order kinetics model for degradation of DR16 at different experimental conditions (pH = 6.8, DR16 dosage = 20 ppm, NaOCl dosage = 0.4 ml/L,  $P = 5$  bar)

Method	$k_1$ (1/min)	$R^2$
HC	0.0087	0.7294
UV	0.0068	0.9703
NaOCl	0.0423	0.9225
HC + UV	0.0209	0.7787
HC + NaOCl	0.0581	0.7214
UV + NaOCl	0.0522	0.9259
HC + UV + NaOCl	0.0805	0.8020

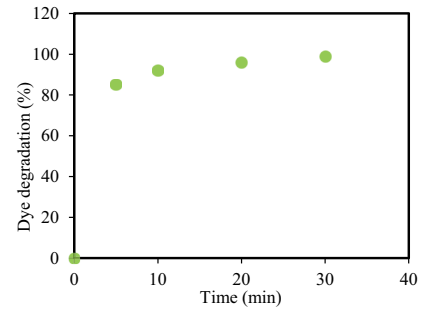


Fig. S1. Degradation of DR16 (solved in deionized water) at (pH = 6.8, DR16 dosage = 20 ppm, DR16/NaOCl molar ratio of 1:20,  $P = 5$  bar).